# *Synthesis and characteristics study of $TiO_2$ nanowires and nanoflowers on FTO/glass and glass substrates via hydrothermal technique*

**Abdul Qader Dawood Faisal**

**Journal of Materials Science: Materials in Electronics**

ISSN 0957-4522
Volume 26
Number 1

J Mater Sci: Mater Electron (2015)
26:317-321
DOI 10.1007/s10854-014-2402-4

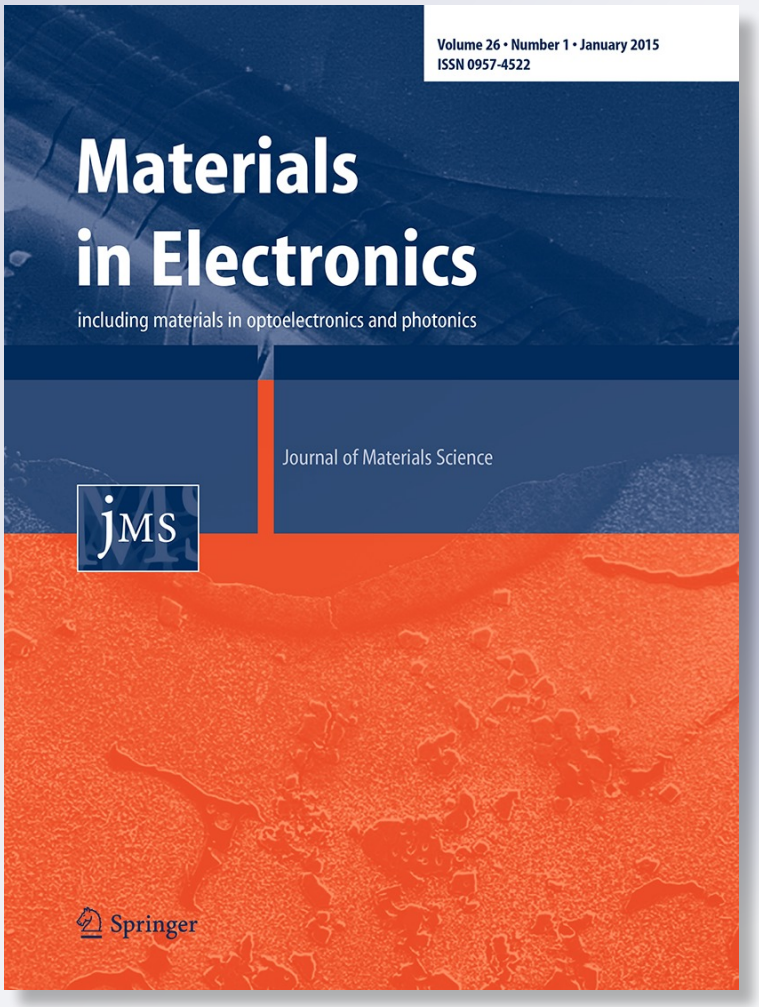


Springer

J Mater Sci: Mater Electron (2015) 26:317–321
DOI 10.1007/s10854-014-2402-4

# Synthesis and characteristics study of $TiO_2$ nanowires and nanoflowers on FTO/glass and glass substrates via hydrothermal technique

**Abdul Qader Dawood Faisal**

Received: 3 September 2014 / Accepted: 10 October 2014 / Published online: 7 November 2014


**Abstract** In this work, a typical hydrothermal synthesis to grow long, high density, vertically aligned, well oriented and homogenous $TiO_2$ nanowires arrays and flower-like film on conductive and nonconductive (glass) sides of fluorine doped tin oxide (FTO-glass) substrate are presented. Under the same conditions, the $TiO_2$ nanowires arrays were directly grown on the FTO coated side. While the flower-like nanostructures were grown on the glass side. Two cleaned FTO-glass samples were placed inside the autoclave cylinder. The samples were placed at horizontal and inclined at 45° respectively. The average diameter and length of nanowires are 150 nm and 7.0 μm respectively. Also the average diameter of the prepared flower-like nanostructure of $TiO_2$ is ≈5–10 μm. The flower-like nanostructure growth was confirmed in the absence of FTO by scratched line made on conductive side. The optical propertied of the $TiO_2$ flower-like nanostructures was also investigated. The synthesized products were characterized by SEM equipped with EDS, XRD and UV–VIS NIR spectrophotometer.

## 1 Introduction

Titanium dioxide ($TiO_2$) is considered as promising material for different applications due to their photoinduced reactivity and electronic properties. $TiO_2$ is stable, cheap, and nontoxic, exist in three crystalline forms: rutile (Eg = 3.05 eV) [1], anatas (Eg = 3.32 eV) [2] and brookite (3.26 eV) [3]. Typically, Titanium dioxide exists in three crystalline structures: rutile (tetragonal), anatase (tetragonal) and brookite (orthorhombic). Rutile is a stable form, whereas anatase and brookite are metastable and are readily converted to rutile when heated [4, 5]. In recent years, a variety of synthesis methods of $TiO_2$ nanostructures have been used such as solvothermal [6], sol–gel [7], thermal oxidation [8], chemical vapor deposition (CVD) [9], spray pyrolysis [10], sonochemical method [11], and hydrothermal [12, 13] and microwave assisted hydrothermal [14, 15] have been used for the preparation of $TiO_2$ nanostructured. The morphologies of $TiO_2$ have mainly included nanostructures such as Nanoparticles [16], Nanotubes [17–19], Nanowires (NWs) [20], Nanorods [21], Nanoflowers (NFs) [22], and Nanobelt [23]. However, hydrothermal technique is one of the most convenient and effective method for preparation of metal oxide nanostructures like $TiO_2$. The required superior properties can be achieved easily by varying the hydrothermal experimental condition. Metal oxide materials such as $TiO_2$ nanostructures have been extensively studied for various applications such as: Gas sensors [24, 25], Hydrogen generation [26], Dye sensitized solar cells [27] and Lithium-ion battery [28]. In the present work, $TiO_2$ NWs, and NFs were successfully grown directly onto transparent conductive fluorine-doped tin oxide (FTO) substrates side and on nonconductive side using hydrothermal method. A detailed surface morphological and structural characterization were investigated. The morphological removal effect of conductive FTO on the growth of nanostructure of $TiO_2$ was also studied. The optical properties of $TiO_2$ nanostructures were discussed.

## 2 Experimental details

### 2.1 FTO-glass substrate cleaning

In atypical synthesis, two pieces of FTO substrates with sizes 2.5 × 1 $cm^2$, 14Ω/$cm^2$, (Hartford Glass Company)

A. Q. D. Faisal (✉)
Applied Science Department, University of Technology, Baghdad, Iraq
e-mail: adfalobaidi@yahoo.com

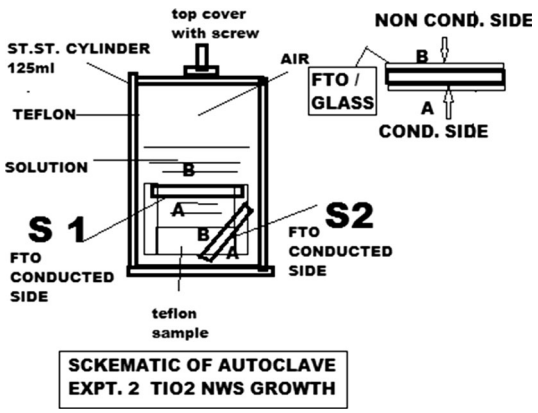


**Fig. 1** Schematic diagram of stainless steel autoclave cylinder and FTO/glass substrate

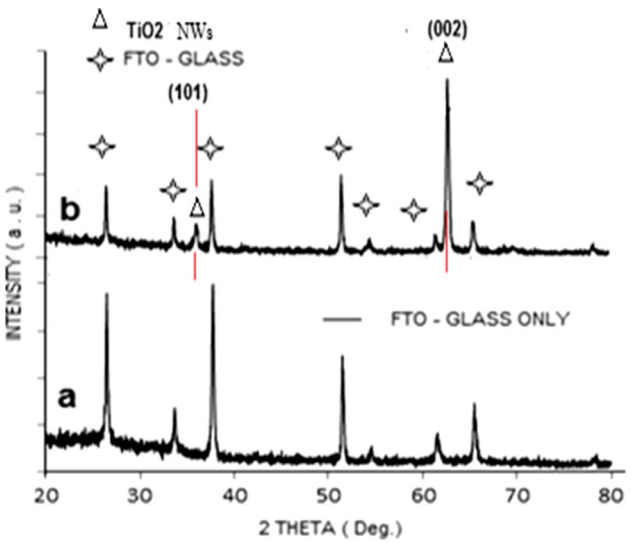


**Fig. 2** XRD patterns of the FTO-glass substrate **a** before hydrothermal growth and **b** after hydrothermal growth

was ultrasonically cleaned for 60 min in a mixed solution of acetone, isopropyl alcohol (IPA), and deionized (DI) water with volume ratio of 1:1:1 and fully dried under $N_2$ flow.

### 2.2 Growth of $TiO_2$ nanwires and nanoflowers

$TiO_2$ NWs and NFs films were grown on both sides of FTO glass substrates using hydrothermal method. The hydrothermal synthesis of $TiO_2$ (NWs) and (NFs) was carried out in a Teflon-lined stainless steel autoclave. Titanium (IV) Butoxide (Aldrich) solution was used as a precursor for the production of $TiO_2$ films. In atypical synthesis process, 30 mL of DI water was mixed with 30 mL of concentrated hydrochloric acid (36.5–38 % by weight to reach a total volume of 60 mL in Teflon-lined stainless steel autoclave (125 mL). The mixture was stirred at ambient conditions for 10 min.Then 1 mL of Ti(IV) butoxide was added to the previous mixture and stirring for another 10 min. Finally, the resulting solution was transferred into an autoclave. Here FTO/coated glass side, and other non-conducting glass side was considered as two substrates referred as A and B respectively as shown in Fig. 1. Two pieces of cleaned FTO/glass were located inside the Teflon cylinder as shown in Fig. 1. One is positioned horizontally on Teflon holder and the other was placed at 45° against the wall of the autoclave (inside Teflon surface), bear in mind that the conductive sides are always down words as shown in Fig. 1. The synthesis was carried out for 20 h in electrical oven at 150 °C. After completion of the reaction, the autoclave was cooled down to room temperature. Finally, the substrates were thoroughly washed with DI water, followed by drying overnight at ambient atmosphere.

### 2.3 Characterization techniques

The crystal structures of $TiO_2$ films were characterized by X-ray diffractometer (XRD/PANalytical, X'Pert) with CuKα (λ = 0.01546 nm) radiation. The surface morphologies of the $TiO_2$ films were observed by scanning electron microscope (SEM/JEOL – JSM 5140) operated at 30 kV and equipped with energy dispersive X-ray spectrometer (EDS).Transmission through the film was measured using UV–vis–NIR spectrophotometer (CARY-500 Scan Varian-USA).

## 3 Results and discussion

### 3.1 XRD analysis for FTO-glass before and after hydrothermal growth

XDR shows that the film as deposited on the conductive side of FTO-glass substrates are rutile $TiO_2$. Figure 2 displays the XRD patterns of FTO-glass substrate before (Fig. 2a) and after (Fig. 2b) the hydrothermal growth. By eliminating the peaks originating from the FTO conductive glass (Fig. 2a), all the diffraction peaks at 36.07° (101) and at 62.810° (002) that appear upon NWs growth films agree well with the tetragonal rutile structure (JCPDS # 65-0191) and confirmed by other workers [29]. The high intensity of (002) diffraction peak originate from $TiO_2$ NWs, which indicates that the as-deposited film is highly oriented with respect to the substrate surface as shown in Fig. 2. That's because of small lattice mismatch between tetragonal FTO (a = b = 0.4687 nm [30]) and rutile TiO2

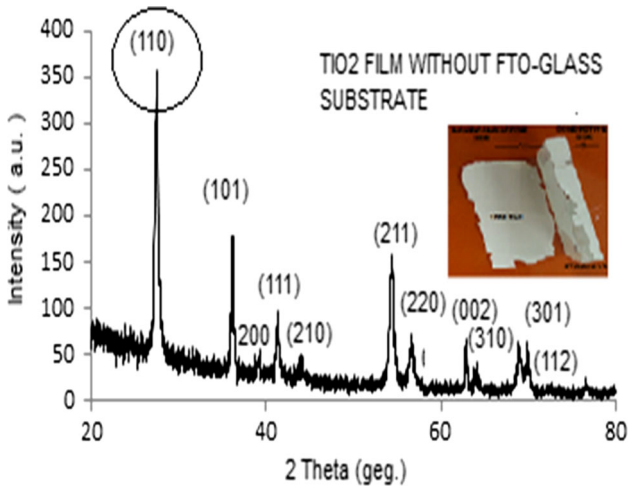


**Fig. 3** The corresponding XRD pattern of $TiO_2$ microspheres without FTO/glass substrate. All the *peaks* are indexed as JCPDS #21–1276 for rutile structure

(a = b = 0.4594 [31]), which promotes the epitaxial nucleation and growth of rutile $TiO_2$. The epitaxial relation between the FTO substrate and rutile $TiO_2$ with a small lattice mismatch plays a key role in driving the nucleation and growth of the rutile $TiO_2$ NWs on FTO.

### 3.2 X-ray diffraction analysis for white thick film only

Figure 3 shows the XRD patterns of $TiO_2$ films as prepared. A very strong diffraction peaks are observed at 2θ of 27.43° (110), 36.17° (101), and 54.43° (211) indicating $TiO_2$ in rutile phase. All peaks are in good agreement with the standard spectrum (JCPDS # 21-1276). This means that rutile is the main crystallographic phase, and they coincide well with the reported value [32].

### 3.3 SEM and EDS analysis of $TiO_2$ NWs and nanoflowers films

Figure 4 shows the typical SEM images of the TiO2 NWs film as synthetized by hydrothermal process. It is clear that the entire surface of the FTO substrate is covered uniformly, are relatively smooth and dense $TiO_2$ NWs as shown in Fig. 4a. The cross-sectional view of such vertically aligned array is shown in the inset (Fig. 4b). The average diameter and length of NWs are 150 nm and 7.0 μm respectively. The calculated aspect ratio is approximately equal to 47.

Figure 5 shows atypical SEM image of the as prepared $TiO_2$ NFs. The SEM image indicate that the NFs are quite clean with no contamination attached to their surface. That's confirmed by EDS measurements shown in Fig. 6. The synthesized rutile $TiO_2$ NFs shown in Fig. 5 are consists of a bunch of aligned nanorods with uniform size and having different orientations.

The $TiO_2$ NFs on glass side can be peeled off as white thick film, while the NWs growth was found to be tightly stick on the conductive side of FTO. That could be due to the interaction between $TiO_2$ NWs and FTO substrate was supported favorable because of electron gravity and nucleation of fluorine in FTO substrate. The thick film about 100 μm of $TiO_2$ film of NFs was analyzed by EDS, which is carried out during SEM analysis. Figure 6 shows only the titanium and oxygen peaks. The peak marked with C (carbon tape base). This implies that the synthesized product film at low temperature is free of contaminations.

### 3.4 $TiO_2$ nanostructures grown on scratched FTO/glass substrate

To confirm the growth of flower-like nanostructure on the glass side of the FTO substrate, deep scratch was made on

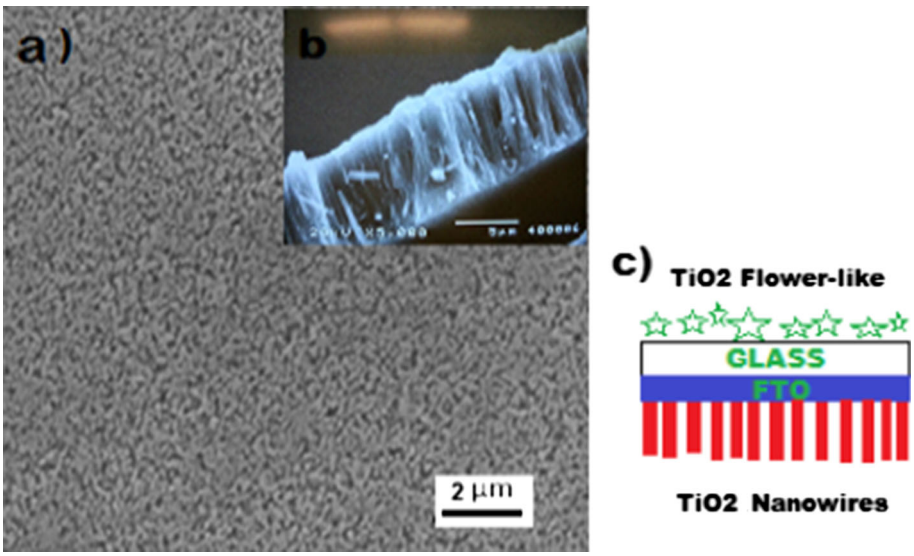


**Fig. 4** **a** *Top view* of the $TiO_2$ nanowires as synthetized on FTO by hydrothermal process, and **b** corresponding cross section view of the film, prepared with reaction time of 20 h and at a reaction temperature of 150 °C (placed at 45°) and **c** growth type on both sides of FTO-glass

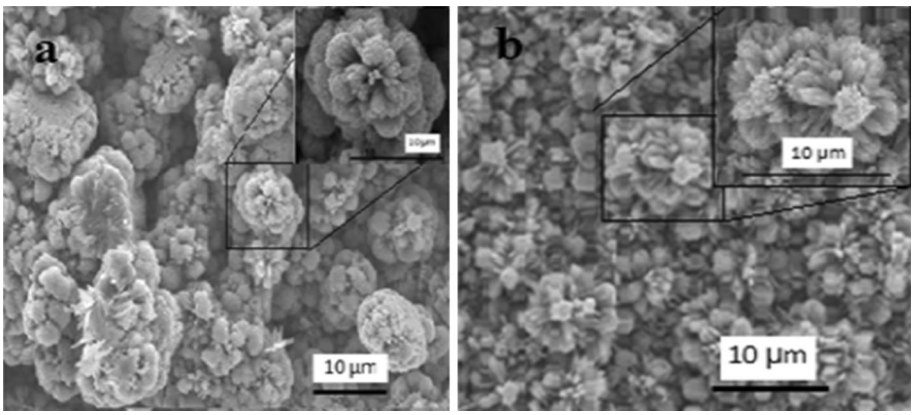


**Fig. 5** SEM images of $TiO_2$ nanoflowers on FTO-glass substrate

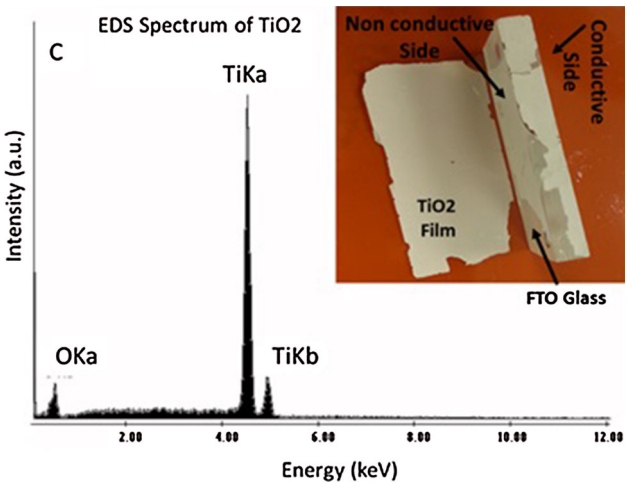


**Fig. 6** EDS analysis of as synthesized $TiO_2$ flower-like nanostructure film

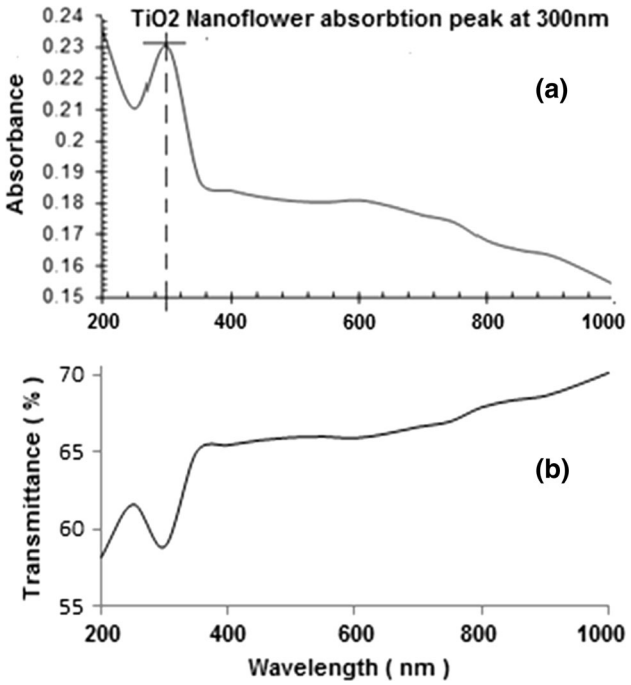


**Fig. 7** Optical absorbance and transmittance spectra of $TiO_2$ film as prepared

the conductive side of FTO, before the growth process and the sample was loaded in autoclave for growth at 150 °C and for 20 h in oven. The results obtained are similar to the reported data in this paper.

## 4 Optical properties of $TiO_2$ film

To study the optical properties of thick white film of $TiO_2$ NFs produced. Small piece of white film shown in Fig. 6 was grinded to a fine powder using ceramic mortar and dissolve in isopropanol for UV–vis analysis. The optical band gap of flower-like (thick white film) for $TiO_2$ estimated from the optical properties in the range between 200 and 1000 nm. Figure 7a shows UV–vis spectrum and a single absorption strong peak at 300 nm peak at about 300 nm in the UV range was noticed. Figure 7a shows UV–vis absorption single strong peak at 300 nm peak at about 300 nm in the UV range. Figure 7(b) shows the transmittance spectrum of $TiO_2$ flower-like film synthesized at 150 °C for 20 h. The transmittance of $TiO_2$ film is shown in Fig. 7b. The average optical transmittance of $TiO_2$ film in the visible range (400–700 nm) is estimated as 65–70 %.

The optical band gap direct allowed transmission was calculated by using Tauc law [33]:

$$\alpha h\nu = C(h\nu - E_g)^{1/2}$$

where α, hν, C and $E_g$ are the absorption coefficient, incident photon energy,constant and direct band gap respectively. The plot of hν versus $(\alpha h\nu)^2$ is shown in Fig. 8. The experimental optical band gap of $TiO_2$ film ($E_g = 3.05 \pm 0.05$ eV) was found for rutile structure

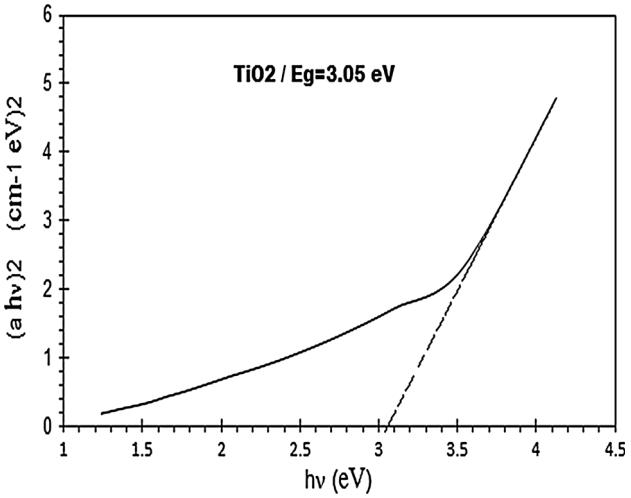


**Fig. 8** Plot of hν versus $(\alpha h\nu)^2$ for $TiO_2$ film as prepared

which was confirmed by XRD (Fig. 3). This energy gap value is quite close to that obtained by other workers [34–36]. The band gaps effectively place the absorption spectrum of pure $TiO_2$ within the ultraviolet range ($\lambda \approx$ 10–400 nm).

## 5 Conclusion

Nanowires and flower-like Titanium dioxide films of rutile phase were successfully synthesized by hydrothermal method. The NWs were grown long, dense, homogenous and vertically aligned on substrate. The process confirmed the growth of NWs on conductive side of FTO side and flower-like on glass side even when the FTO positioned at different angles. The as synthesized nanostructured mainly consisted of $TiO_2$ in rutile phase only. Potential applications of these nanostructures are in solar cells, gas sensors, optoelectronics etc.

**Acknowledgments** I would like to acknowledge Dr. W. Zhou and his group working at AMRI/UNO/New Orleans/Louisiana/USA for laboratories accesses. My special appreciation to the CRDF/ISFP for providing this research opportunity in USA's university.

## References

1. T.E. Tiwald, M. Schubert, Proc. SPIE **4103**, 19 (2000)
2. J.G. Li, T. Ishigaki, X.D. Sun, J. Phys. Chem. **C111**, 4969 (2007)
3. N. Hosaka, T. Sekiya, C. Satoko, S. Kurita, J. Phys. Soc. Japan **66**, 877 (1997)
4. A.D. Paola, G. Cufalo, M. Addamo, M. Bellardita, R. Campostrini, M. Ischia, R. Ceccato, L. Palmisano, Colloid Surf. A Physicochem. Eng. Asp. **317**, 366 (2008)
5. G.L. Puma, A. Bono, D. Krishnaiah, J.G. Collin, J. Haz. Mat. **157**, 209 (2008)
6. Z. Wei, Y. Yao, T. Huang, A. Yu, Int. J. Electrochem. Sci. **6**, 2011 (1879)
7. J.Y. Kim, H.S. Jung, J.H. No et al., J. Electroceram. **16**, 447 (2006)
8. D. Kaewsai, W. Jaruwongjinda, S. Daothong, P. Singjai, A. Watcharapasorn, S. Jiansirisomboon, J. Microsc. Soc. Thailand **24**(2), 145 (2010)
9. L. Liyou, J. Chen, L. Li, W. Wang, Nanoscale Res. Lett. **7**, 293 (2012)
10. I. Oja, A. Mere, M. Krunks et al., Thin Solid Films **515**, 674 (2006)
11. H. Arami, M. Mazloumi, R. Khalifehzadeh, S.K. Sadrnezhaad, Mater. Lett. **61**, 4559 (2007)
12. A. Hu, X. Zhang, K.D. Oakes, P. Peng, Y.N. Zhou, M. R. Servos **189**, 278 (2011)
13. H.-E. Wang, Z. Chen, Y.H. Leung, C. Luan, C. Liu, Y. Tang, C. Yan, W. Zhang, J.A. Zapien, I. Bello, S.T. Lee, Appl. Phys. Lett. **96**, 263104 (2010)
14. L. Cui, K.N. Hui, S. Hui, S.K. Lee, W. Zhou, Z.P. Wan, C.N.H. Thuc, Mater. Lett. **75**, 175 (2012)
15. C.C. Chung, T.W. Chung, T.C.K. Yang, Ind. Eng. Chem. Res. **47**, 2301 (2008)
16. R. Mohan, J. Drbohlavova, J. Hubale, Nanoscale Res. Lett. **8**, 503 (2013)
17. L.X. Yang, S.L. Luo, R.H. Liu, Q.Y. Cai, Y. Xiao, S.H. Liu, F. Su, L.F. Wen, J. Phys. Chem. **C114**, 4783 (2010)
18. Z.Y. Liu, M. Misra, Nanotechnology **21**, 125703 (2010)
19. L. Cui, K.N. Hui, K.S. Hui, S.K. Lee, W. Zhou, Z.P. Wan, C.-N. Ha Thuc, Mater. Lett. **75**, 175 (2012)
20. Z-j Zhou, J-q Fan, X. Wang, W-h Zhou, Z-l Du, S-x Wu, Appl. Mater. Interfaces **3**(11), 4349 (2011)
21. T.A. Kandiel, R. Dillert, A. Feldhoff, D.W. Bahnemann, J. Phys. Chem. **C114**, 4909 (2010)
22. J.M. Wu, B. Qi, J. Phys. Chem. **C111**, 666 (2007)
23. D. Pradhan, Z. Su, S. Sindhwani, J.F. Honek, K.T. Leung, J. Phys. Chem. C **115**(37), 18149 (2011)
24. W.C. Tian, Y.H. Ho, C.H. Chen, C.Y. Kuo, Sensors **13**, 865 (2013)
25. M. Munz, M. Langridge, K. Devarepally, D.C. Cox, P. Patel, N. Martin, G.M. Vargha, V. Stolojan, S. White, R.J. Curry, Appl. Mater. Interfaces **5**(4), 1197 (2013)
26. T.N. Ravishankar, K. Manjunatha, S. Sarkar, H. Nagabhushana, R. Goncalves, J. Dupont, Mater. Lett. **109**, 27 (2013)
27. C.Z. Shen, X. Zhang, Y. Wang, B.A. Korgel, A. Gupta, N. Bao, Appl. Mater. Interfaces **6**(1), 122 (2014)
28. H. Qiao, Q. Luo, Q. Wei, Y. Cai, F. Huang, Ionics **18**, 667 (2012)
29. B. Liu, E.S. Aydil, J. Am. Chem. Soc. **131**(11), 3985 (2009)
30. M. Abd-Lefdil, R. Diaz, H. Bihri, M.A. Aouaj, F. Rueda, Eur. Phys. J. Appl. Phys. **38**(3), 217 (2007)
31. C.J. Howard, T.M. Sabine, F. Dickson, Acta Crystallogr. Sect. B **47**, 462 (1991)
32. A. Kumar, A.R. Madaria, C. Zhou, J. Phys. Chem. C **114**, 7787 (2010)
33. S. Venkatachalam, D. Mangalaraj, S.A.K. Narayandass, Phys. B **393**, 47 (2007)
34. J.-C. Lee, K.-S. Park, T.-G. Kim, H.-J. Choi, Y.-M. Sung, Nanotechnology **17**, 4317 (2006)
35. D.P. Macwan, P.N. Dave, J. Mater. Sci. **46**, 3669 (2011)
36. R. Mohan, J. Drbohlavova, J. Hubalek, Nanoscale Res. Lett. **8**, 530 (2013)